Improved transmission model for metal-dielectric-metal plasmonic waveguides with stub structure

Asanka Pannipitiya,[1,*] **Ivan D. Rukhlenko,**[1] **Malin Premaratne,**[1]
Haroldo T. Hattori,[2] **and Govind P. Agrawal**[3]

[1]*Advanced Computing and Simulation Laboratory (AχL)*
Department of Electrical and Computer Systems Engineering
Monash University, Melbourne, VIC 3800, Australia
[2]*SEIT, University of New South Wales*
Australian Defence Force Academy, Canberra, ACT 2600, Australia
[3]*Institute of Optics, University of Rochester, Rochester, NY 14627, USA*
asanka.pannipitiya@eng.monash.edu.au

Abstract: We present an improved analytical model describing transmittance of a metal-dielectric-metal (MDM) waveguide coupled to an arbitrary number of stubs. The model is built on the well-known analogy between MDM waveguides and microwave transmission lines. This analogy allows one to establish equivalent networks for different MDM-waveguide geometries and to calculate their optical transmission spectra using standard analytical tools of transmission-line theory. A substantial advantage of our model compared to earlier works is that it precisely incorporates the dissipation of surface plasmon polaritons resulting from ohmic losses inside any metal at optical frequencies. We derive analytical expressions for transmittance of MDM waveguides coupled to single and double stubs as well as to N identical stubs with a periodic arrangement. We show that certain phase-matching conditions must be satisfied to provide optimal filtering characteristics for such waveguides. To check the accuracy of our model, its results are compared with numerical data obtained from the full-blown finite-difference time-domain simulations. Close agreement between the two suggests that our analytical model is suitable for rapid design optimization of MDM-waveguide-based compact photonic devices.

OCIS codes: (240.6680) Surface plasmons; (230.7400) Waveguides, slab; (250.5300) Photonic integrated circuits; (260.2110) Electromagnetic optics; (130.2790) Guided waves.

References and links

1. W. L. Barnes, A. Dereux, and T. W. Ebbesen, "Surface plasmon subwavelength optics," Nature **424**, 824-830 (2003).
2. W. L. Barnes, "Surface plasmon-polariton length scales: A route to sub-wavelength optics," J. Opt. A: Pure Appl. Opt. **8**, S87-S93 (2006).
3. S. A. Maier, P. G. Kik, and H. A. Atwater, "Optical pulse propagation in metal nanoparticle chain waveguides," Phys. Rev. B **67**, 205402(1-5) (2003).
4. S. A. Maier, P. G. Kik, H. A. Atwater, S. Meltzer, E. Harel, B. E. Koel, and A. G. Requicha, "Local detection of electromagnetic energy transport below the diffraction limit in metal nanoparticle plasmon waveguides," Nature **2**, 229-232 (2003).
5. W. H. Weber and G. W. Ford, "Propagation of optical excitations by dipolar interactions in metal nanoparticle chains," Phys. Rev. B **70**, 125409(1-8) (2004).

#123889 - $15.00 USD Received 5 Feb 2010; revised 23 Feb 2010; accepted 8 Mar 2010; published 11 Mar 2010

6. K. Leosson, T. Nikolajsen, A. Boltasseva, and S. I. Bozhevolnyi, "Long-range surface plasmon polariton nanowire waveguides for device applications," Opt. Express **14**, 314-319 (2006).
7. V. A. Podolskiy, A. K. Sarychev, E. E. Narimanov, and V. M. Shalaev, "Resonant light interaction with plasmonic nanowire systems," J. Opt. A: Pure Appl. Opt. **7**, S32-S37 (2005).
8. J. Takahara, S. Yamagishi, H. Taki, A. Morimoto, and T. Kobayashi, "Guiding of a one-dimensional optical beam with nanometer diameter," Opt. Lett. **22**, 475-477 (1997).
9. S. A. Maier and H. A. Atwater, "Plasmonics: Localization and guiding of electromagnetic energy in metal/dielectric structures," J. Appl. Phys. **98**, 011101(1-10) (2005).
10. G. Veronis and S. Fan, "Modes of subwavelength plasmonic slot waveguides," J. Lightwave Technol. **25**, 2511-2521 (2007).
11. F. I. Baida, A. Belkhir, D. V. Labeke, and O. Lamrous, "Subwavelength metallic coaxial waveguides in the optical range: Role of the plasmonic modes," Phys. Rev. B **74**, 205419(1-7) (2006).
12. S. I. Bozhevolnyi, V. S. Volkov, E. Devaux, and T. W. Ebbesen, "Channel plasmon-polariton guiding by subwavelength metal grooves," Phys. Rev. Lett. **95**, 046802(1-4) (2005).
13. D. F. P. Pile, T. Ogawa, D. K. Gramotnev, T. Okamoto, M. Haraguchi, M. Fukui, and S. Matsuo, "Theoretical and experimental investigation of strongly localized plasmons on triangular metal wedges for subwavelength waveguiding," Appl. Phys. Lett. **87**, 061106(1-3) (2005).
14. G. Veronis and S. Fan, "Bends and splitters in metal-dielectric-metal subwavelength plasmonic waveguides," Appl. Phys. Lett. **87**, 131102(1-3) (2005).
15. T. Lee and S. Gray, "Subwavelength light bending by metal slit structures," Opt. Express **13**, 9652-9659 (2005).
16. H. Gao, H. Shi, C. Wang, C. Du, X. Luo, Q. Deng, Y. Lv, X. Lin, and H. Yao, "Surface plasmon polariton propagation and combination in Y-shaped metallic channels," Opt. Express **13**, 10795-10800 (2005).
17. G. Veronis and S. Fan, "Theoretical investigation of compact couplers between dielectric slab waveguides and two-dimensional metal-dielectric-metal plasmonic waveguides," Opt. Express **15**, 1211-1221 (2007).
18. R. A. Wahsheh, Z. Lu, and M. A. G. Abushagur, "Nanoplasmonic couplers and splitters," Opt. Express **17**, 19033-19040 (2009).
19. E. N. Economou, "Surface plasmons in thin films," Phys. Rev. **182**, 539-554 (1969).
20. B. Prade, J. Y. Vinet, and A. Mysyrowicz, "Guided optical waves in planar heterostructures with negative dielectric constant," Phys. Rev. B **44**, 13556-13572 (1991).
21. G. Veronis and S. Fan, "Subwavelength plasmonic waveguide structures based on slots in thin metal films," in *Integrated Optics: Devices, Materials, and Technologies X*, Y. Sidorin and C. A. Waechter, eds., Proc. SPIE **6123**, 612308(1-10) (2006).
22. X. Lin and X. Huang, "Tooth-shaped plasmonic waveguide filter with nanometric sizes," Opt. Lett. **33**, 2874-2876 (2008).
23. J. Tao, X. Huang, X. Lin, Q. Zhang, and X. Jin, "A narrow-band subwavelength plasmonic waveguide filter with asymmetrical multiple-teeth-shaped structure," Opt. Express **17**, 13989-13994 (2009).
24. X. Lin and X. Huang, "Numerical modeling of a teeth-shaped nanoplasmonic waveguide filter," J. Opt. Soc. Am. B **26**, 1263-1268 (2009).
25. Y. Matsuzaki, T. Okamoto, M. Haraguchi, M. Fukui, and M. Nakagaki, "Characteristics of gap plasmon waveguide with stub structures," Opt. Express **16**, 16314-16325 (2008).
26. J. Tao, X. G. Huang, J. Chen, Q. Zhang, and X. Jin, "Systematical research on characteristics of double-sided teeth-shaped nanoplasmonic waveguide filters," J. Opt. Soc. Am. B **27**, 323-327 (2010).
27. J. Liu, G. Fang, H. Zhao, Y. Zhang, and S. Liu, "Surface plasmon reflector based on serial stub structure," Opt. Express **17**, 20134-20139 (2009).
28. S. E. Kocabas, G. Veronis, D. A. B. Miller, and S. Fan, "Transmission line and equivalent circuit models for plasmonic waveguide components," IEEE J. Sel. Top. Quantum Electron. **14**, 1462-1472 (2008).
29. G. Veronis, S. E. Kocabas, D. A. B. Miller, and S. Fan, "Modeling of plasmonic waveguide components and networks," J. Comput. Theor. Nanosci. **6**, 1808-1826 (2009).
30. P. A. Rizzi, *Microwave Engineering: Passive Circuits* (Prentice-Hall, New Jersey, 1988).
31. S. Ramo, J. R. Whinnery, and T. V. Duzer, *Fields and Waves in Communication Electronics*, 3rd ed. (Wiley, New York, 1994).
32. D. M. Pozar, *Microwave Engineering*, 2nd ed. (Wiley, New York, 1998).
33. S. A. Maier, *Plasmonics: Fundamentals and Applications* (Springer Science, 2007).
34. J. A. Dionne, L. A. Sweatlock, H. A. Atwater, and A. Polman, "Plasmon slot waveguides: Towards chipscale propagation with subwavelength-scale localization," Phys. Rev. B **73**, 035407(1-9) (2006).
35. K. Y. Kim, Y. K. Cho, H.-S. Tae, and J.-H. Lee, "Light transmission along dispersive plasmonic gap and its subwavelength guidance characteristics," Opt. Express **14**, 320-330 (2006).
36. A. D. Rakic, A. B. Djurisic, J. M. Elazar, and M. L. Majewski, "Optical properties of metallic films for vertical-cavity optoelectronic devices," Appl. Opt. **37**, 5271-5283 (1998).
37. E. D. Palik, *Handbook of Optical Constants of Solids* (Academic , New York, 1985).
38. K. Zhang and D. Li, *Electromagnetic Theory for Microwaves and Optoelectronics*, 2nd ed. (Springer, Berlin, 2008).

#123889 - $15.00 USD Received 5 Feb 2010; revised 23 Feb 2010; accepted 8 Mar 2010; published 11 Mar 2010

39. M. A. Parker, *Physics of Optoelectronics* (CRC Press, Florida, 2005).

1. Introduction

Plasmonic waveguides have attracted considerable attention in recent years because of their ability to provide subwavelength optical confinement resulting from the strong localization of surface plasmon polaritons (SPPs) at metal-dielectric interfaces [1, 2]. Some of the promising SPP-guiding geometries include arrayed nanoparticles [3–5], nanowires [6–8], metal-dielectric-metal (MDM) waveguides [9–11], V-grooves, [12], and wedges [13]. In the case of MDM waveguides, their capacity to sustain SPP modes with nanoscale effective areas opens up many possibilities for a wide range of applications including power splitters [14], U-shaped waveguides [15], Y-shaped combiners [16], and waveguide couplers [17, 18]. For this reason, a great deal of effort is currently being devoted to develop MDM-waveguide-based optical components, similar to those already available at microwave and radio frequencies. Owing to their compact size, these components are promising candidates for future devices required for nanoscale integrated optics [19–21].

One of the most challenging applications of MDM waveguides is the wavelength-selective optical filter (or reflector), which is implemented by coupling one or more stubs perpendicular to the waveguide axis [22–24]. Transmission spectrum of such filters can be controlled by varying the number of stubs and/or their parameters such as length, width, and positions. The MDM-waveguide-based optical filters are commonly modeled by solving Maxwell's equations with the finite-difference time-domain (FDTD) scheme [22–26]. Another way to model such filters is to employ the analogy between MDM heterostructures and microwave transmission lines [14, 25, 27–29]. This analogy allows one to utilize network-analysis tools to calculate transmittance for simple filter geometries analytically [30–32]. Since the latter method has been developed for lossless waveguides [25, 27], it is unable to produce accurate results for lossy waveguides and hence needs to be supplemented with numerically-calculated parameters to enhance the accuracy [24]. Since calculation of the filter transmission spectrum with the current methods is either time-consuming or inaccurate, it is difficult to perform device optimization. Clearly, a purely analytical description of MDM-waveguide-based optical filters that allows for SPP damping will be of considerable practical importance.

In this work, for the first time to the best of our knowledge, we develop an improved analytical model for dissipative MDM waveguides with stub structure. The paper is organized as follows. In Section 2, we introduce the dispersion law of SPPs that governs major properties of a plasmonic waveguide. In Section 3, using physical similarity, we establish relationships between the parameters of MDM waveguide coupled to one stub and characteristic impedances of an equivalent transmission line. By application of standard transmission line theory, we then derive analytical expressions for the transmission spectra of the waveguide coupled to one and two stubs. An algorithm for calculating the transmittance in the case of an arbitrary stub structure is developed in Section 4. Using this algorithm, we evaluate analytically the transmittance of an MDM waveguide coupled to an arbitrary number of periodically arranged stubs. Main results of the paper are summarized in Section 5.

2. Dispersion relation for MDM waveguides

We briefly review the results of MDM-waveguide theory that will be used in the following section. Consider a planar MDM waveguide consisting of a dielectric layer of thickness h surrounded by two metallic layers that thick enough that they can be assumed to extend to infinity (see Fig. 1). It is well known that each of metal-dielectric interfaces at $y = \pm h/2$ supports a localized transverse-magnetic (TM) SPP mode propagating along the x direction. If the distance

#123889 - $15.00 USD Received 5 Feb 2010; revised 23 Feb 2010; accepted 8 Mar 2010; published 11 Mar 2010

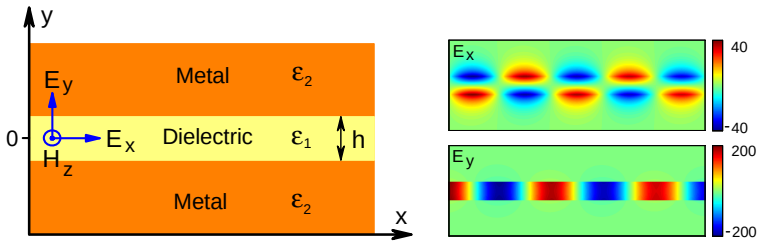

Fig. 1. Left panel: Schematic of an MDM waveguide with dielectric layer of thickness h and permittivity ε_1 separating two metallic layers of permittivity ε_2. Right panel: Density plots of longitudinal (E_x) and transverse (E_y) electric fields (in arbitrary units) corresponding to the fundamental antisymmetric SPP mode.

between the interfaces is comparable to or smaller than the skin depth of SPPs in dielectric, the localized modes become coupled [33]. The coupled SPP modes of frequency ω are described by the electromagnetic field components $U_j(x,y,t) \equiv \{E_{jx}, E_{jy}, H_{jz}\}$, whose evolution in the propagation direction x is governed by the complex-valued propagation constant β such that

$$U_j(x,y,t) = U_j(y)\exp[i(\beta x - \omega t)],$$

where $j = 1$ in the dielectric layer and 2 in each metal layer.

The effective refractive index n_{eff} of an MDM waveguide is also complex. Its real part determines the guided wavelength λ_{MDM} and its imaginary part determines the propagation length L_{SPP} of SPPs through the relation

$$n_{\text{eff}} = \frac{\beta}{k} = \frac{\lambda}{\lambda_{\text{MDM}}} + i\frac{\lambda}{4\pi L_{\text{SPP}}},$$

where $k = 2\pi/\lambda$, $\lambda = 2\pi c/\omega$, and c is the speed of light in vacuum. One can calculate β using the following dispersion relation for the TM-SPP modes [34]:

$$\tanh\left(\frac{ik_1 h}{2}\right) = \left(\frac{\varepsilon_2}{\varepsilon_1}\frac{k_1}{k_2}\right)^{\pm 1}, \tag{1}$$

where the signs $\pm$ correspond to symmetric and antisymmetric modes with $E_x(y) = \pm E_x(-y)$, $k_j = (\varepsilon_j k^2 - \beta^2)^{1/2}$ $(j = 1,2)$, and ε_j is the relative permittivity of the jth medium (see Fig. 1).

Similar to the case of conventional dielectric waveguides, the number of modes supported by an MDM waveguide increases with increasing thickness of the central dielectric layer. Using Eq. (1), one may show that for $h \ll \lambda$, an MDM waveguide supports only a single antisymmetric mode that is similar to the fundamental TEM mode of a parallel-plate waveguide with perfect-electric-conductor (PEC) boundaries [20, 33, 34]: The symmetric mode ceases to exist because it experiences a cut-off in the reciprocal space [35]. Thus, in the deep subwavelength regime, an MDM waveguide operates as a single-mode plasmonic waveguide. Since this regime is the most interesting from the standpoint of nanophotonics applications, we assume in this paper that the condition $h \ll \lambda$ is satisfied and focus on a single-mode plasmonic waveguide.

In Section 3, we illustrate our improved theory of transmission through an MDM waveguide with stub structure using the example of a silver–air–silver waveguide $(\varepsilon_1 = 1)$. To describe the dispersion of silver permittivity, we employ a seven-pole Drude–Lorentz model, known to be reasonably accurate in the wavelength range from 0.2 to 2 μm, and use the expression [36],

$$\varepsilon_2(\omega) = 1 - \frac{\omega_p^2}{\omega(\omega + i\gamma)} + \sum_{n=1}^{5}\frac{f_n\omega_n^2}{\omega_n^2 - \omega^2 - i\omega\gamma_n},$$

#123889 - $15.00 USD Received 5 Feb 2010; revised 23 Feb 2010; accepted 8 Mar 2010; published 11 Mar 2010

Table 1. Parameters of the Drude–Lorentz model for silver

n	ω_n (THz)	γ_n (THz)	f_n
1	197.3	939.62	7.9247
2	1083.5	109.29	0.5013
3	1979.1	15.71	0.0133
4	4392.5	221.49	0.8266
5	9812.1	584.91	1.1133

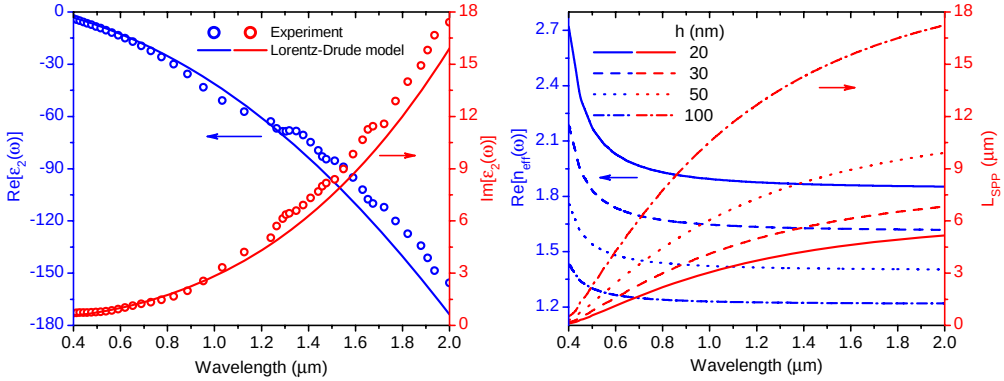

Fig. 2. Left panel: Real and imaginary parts of the dielectric permittivity of silver. Open circles show the experimental data and the solid curves show the fit with the 7-pole Drude–Lorentz model. Right panel: Real part of the effective refractive index and propagation length of SPPs for four thicknesses of the air layer in the Ag–air–Ag-waveguide.

where $\omega_p = 2002.6$ THz is the bulk plasma frequency of silver and $\gamma = 11.61$ THz is a damping constant. The resonant frequencies ω_n, damping constants γ_n, and weights f_n associated with the five Lorentzian peaks are summarized in Table 1.

The left panel in Fig. 2 compares the Drude–Lorentz fit for silver permittivity with the experimental data from Ref. [37]. The right panel shows $\mathrm{Re}(n_{\mathrm{eff}})$ and L_{SPP} as a function of λ, calculated using Eq. (1), for air-layer thicknesses of 20, 30, 50, and 100 nm. As the panel indicates, the guided wavelength is higher for weaker localization of SPPs and decays monotonously with decreasing frequency. It can be also evident that a decrease in h leads to significant reduction in the propagation length of SPPs. This is explained by the increase of electromagnetic energy inside the metal and the resulting growth of ohmic losses. Interestingly, the propagation length is longer at smaller frequencies despite the fact that the corresponding dissipative losses are higher.

3. Transmittance of MDM waveguides with one or two stubs

3.1. *Single-stub case*

Consider the simplest scenario shown in Fig. 3(a) where an MDM waveguide of thickness $h \ll \lambda$ is coupled to a single stub of width w placed perpendicular to the waveguide axis at $x = l$. As seen in Section 2, the properties of MDM waveguide can be characterized by the propagation constant $\beta(h)$ satisfying Eq. (1). If $w \ll \lambda$, we can model the stub by a truncated single-mode MDM waveguide of length d and describe it by a constant $\beta(w)$. To simplify

#123889 - $15.00 USD Received 5 Feb 2010; revised 23 Feb 2010; accepted 8 Mar 2010; published 11 Mar 2010

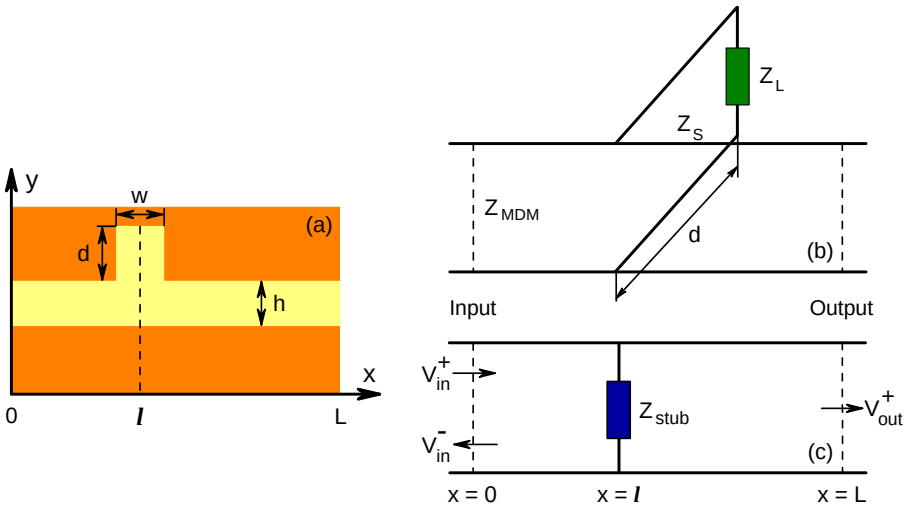

Fig. 3. Schematic of an MDM waveguide with a single stub of width w and length d coupled perpendicular to the waveguide axis (a). The equivalent transmission-line representation (b), its simplified circuit model (c), and details of the notations employed. Z_{MDM} and Z_S are the characteristic impedances of transmission lines corresponding to the MDM waveguide and the stub; Z_L accounts for the reflection of SPPs from the stub end; Z_{stub} is the effective stub impedance.

the following treatment, we neglect the effects associated with fringing fields and higher-order decaying modes excited in the vicinity of the stub-waveguide junction.

To find the transmittance of the waveguide segment between the planes $x = 0$ and $x = L$ [see Fig. 3(a)], we employ the analogy between the subwavelength waveguiding in photonics and electronics [14, 25, 27–29]. With this analogy and the quasi-static approximation (valid as long as $h \ll \lambda$ and $w \ll \lambda$), we can replace the MDM waveguide coupled to a single stub by an equivalent network shown in Fig. 3(b). The network is formed by a parallel connection of an infinite transmission line with the characteristic impedance Z_{MDM} (representing the MDM waveguide) and a finite transmission line with the characteristic impedance Z_S terminated by a load Z_L (representing the stub). The impedance Z_L accounts for the phase shift and the damping of SPP mode caused by its reflection from the end of the stub.

The impedances Z_{MDM}, Z_S, and Z_L need to be expressed in terms of the waveguide parameters h, w, d, $\beta(h)$, $\beta(w)$, ε_1, and ε_2 using clear physical arguments. The analogs of the transverse electric and magnetic fields of the SPP mode are, respectively, the voltage and the current in a transmission line [28, 31, 32]. Using this analogy, the characteristic impedance of the infinite transmission line has the form [14]

$$Z_{\mathrm{MDM}}(h) \approx \frac{E_{1y}h}{H_{1z}} = \frac{\beta(h)h}{\omega\varepsilon_0\varepsilon_1}, \tag{2}$$

where ε_0 is the permittivity of vacuum. In deriving Eq. (2), we took into account the fact that the energy of the SPP mode is mainly confined within the dielectric layer, whereas the distribution of the transverse electromagnetic field is nearly uniform along the y axis (see Fig. 1). Using the same argument, the characteristic impedance of the transmission line representing the stub is given by

$$Z_S(w) = Z_{\mathrm{MDM}}(w) = \frac{\beta(w)w}{\omega\varepsilon_0\varepsilon_1}. \tag{3}$$

#123889 - $15.00 USD Received 5 Feb 2010; revised 23 Feb 2010; accepted 8 Mar 2010; published 11 Mar 2010

The propagation constant $\beta(w)$ is obtained from Eq. (1) after replacing h with w.

To find the value of Z_L, we require it to provide the same amplitude reflectance for electromagnetic wave as the stub end does for the TM-SPP mode. Assuming that SPPs experience normal reflection from the stub end and equating the amplitude reflectance given by the Fresnel's theory [38] to that calculated using circuit analysis [32], we obtain the relation

$$\Gamma = \frac{Z_L - Z_S}{Z_L + Z_S} = \frac{\sqrt{\varepsilon_2} - \sqrt{\varepsilon_1}}{\sqrt{\varepsilon_2} + \sqrt{\varepsilon_1}},$$

which leads to

$$Z_L(w) = \sqrt{\frac{\varepsilon_2}{\varepsilon_1}}\, Z_S(w). \tag{4}$$

Equations (2)–(4) establish the required mapping between the MDM waveguide with one stub and its equivalent network.

Notice that, in the approximation of a perfect electric conductor (PEC) when $|\varepsilon_2| \to \infty$, the amplitude reflectance approaches unity and Z_L tends to infinity. This implies that with regard to the TM-SPPs, the waveguide stub is equivalent to an open circuit rather than to a short-circuited transmission line, as might appear at a glance. The PEC approximation is especially important from methodological point of view, since it reveals the scope of analogy between the MDM waveguides and the transmission lines. Indeed, the transmission-line theory predicts that the reflection from the end of an open circuit does not change the polarity of the voltage, but flips the polarity of the current (see, for example, Eqs. (3.25) and (3.26) in Ref. [38]). On the other hand, the reflection of the TM mode from the PEC boundary conserves the magnetic field vector and inverts the phase of the electric field. Thus there is no analogy between the direction of the electric (magnetic) field of SPPs and the polarity of the voltage (current). This fact is not surprising, for the Maxwell equations are by far more complex than the telegraph equations.

The network scheme in Fig. 3(b) may be redrawn in an equivalent form as shown in Fig. 3(c) by replacing the part corresponding to the stub section by an effective impedance Z_{stub}. The value of Z_{stub} can be obtained from transmission-line theory and is given by [32, 38]

$$Z_{\text{stub}} = Z_S \frac{Z_L - iZ_S \tan(\beta d)}{Z_S - iZ_L \tan(\beta d)}, \tag{5}$$

where $\beta \equiv \beta(w)$.

The transmittance of the simplified network is readily obtained using the transfer matrix method [27, 32, 39]. According to this method, the voltages near the input $(x = 0)$ and output $(x = L)$ ends of the transmission line,

$$V_{\text{in}}(x) = V_{\text{in}}^{+} \exp(i\beta x) + V_{\text{in}}^{-} \exp(-i\beta x), \quad V_{\text{out}}(x) = V_{\text{out}}^{+} \exp[i\beta(x - L)],$$

are related by the matrix equation

$$\begin{pmatrix} V_{\text{in}}^{+} \\ V_{\text{in}}^{-} \end{pmatrix} = \mathbf{T} \begin{pmatrix} V_{\text{out}}^{+} \\ 0 \end{pmatrix}, \tag{6}$$

where the transfer matrix is given by $\mathbf{T} = \mathbf{A}(l)\mathbf{B}(Z_{\text{stub}})\mathbf{A}(L - l)$ with

$$\mathbf{A}(x) = \begin{pmatrix} \exp(-i\beta x) & 0 \\ 0 & \exp(i\beta x) \end{pmatrix}, \quad \mathbf{B}(Z_{\text{stub}}) = \begin{pmatrix} 1 + \dfrac{Z_{\text{MDM}}}{2Z_{\text{stub}}} & \dfrac{Z_{\text{MDM}}}{2Z_{\text{stub}}} \\ -\dfrac{Z_{\text{MDM}}}{2Z_{\text{stub}}} & 1 - \dfrac{Z_{\text{MDM}}}{2Z_{\text{stub}}} \end{pmatrix}. \tag{7}$$

#123889 - $15.00 USD Received 5 Feb 2010; revised 23 Feb 2010; accepted 8 Mar 2010; published 11 Mar 2010

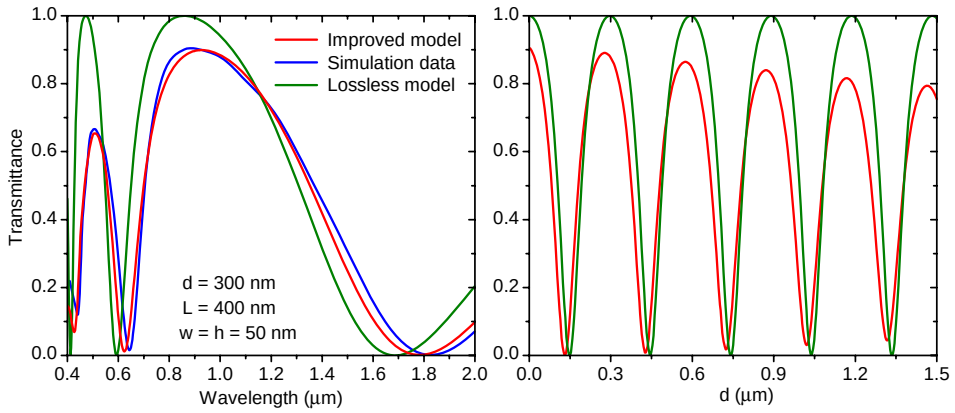

Fig. 4. Transmission spectra of the Ag–air–Ag waveguide coupled to a 300-nm stub (left panel) and the evolution of the waveguide transmittance with the stub length for $\lambda = 850$ nm (right panel). The red, blue, and green curves show the results of our improved model [Eq. (8)], FDTD simulations, and the lossless model, respectively. The waveguide parameters are: $h = w = 50$ nm and $L = 400$ nm.

Physically speaking, the transfer matrix **A** describes wave propagation between the stub and input/output facet of the waveguide, while the matrix **B** represents coupling between the forward- and backward-propagating waves caused by the impedance Z_{stub}.

Using Eqs. (6) and (7), the transmittance of the MDM waveguide coupled to a single stub is found to be

$$T_1 = \left|\frac{V_{\text{out}}^+}{V_{\text{in}}^+}\right|^2 = \left|1 + \frac{Z_{\text{MDM}}}{2Z_{\text{stub}}}\right|^{-2} \exp\left(-\frac{L}{L_{\text{SPP}}}\right). \tag{8}$$

This result has a clear physical structure. The first part with the modulus accounts for interference between the incident wave and the wave reflected from the stub. The exponential factor describes attenuation of SPPs, which is unavoidable in plasmonic waveguides. As one may expect, the signal intensity decays on a length scale of the characteristic propagation length of the SPP mode, $L_{\text{SPP}} = (2\text{Im}\beta)^{-1}$. Note that T_1 does not contain the parameter l, which means that the exact position of the stub within MDM waveguide is unimportant.

A major advantage of our model compared to earlier ones [25, 27] is that it includes automatically the phase shift of SPPs during their reflection from the stub end. This phase shift vanishes for perfect conductors with $\varepsilon_2 = -\infty$. In this limit, Z_L also becomes infinite, and Eq. (8) recovers the well-known result in Ref. [25]. It is also worth noting that the inclusion of the impedance Z_L to represent the phase shift does not prevent us from getting the correct value of T_1 in the absence of the stub. Since the first factor in T_1 approaches 1 when $d \to 0$ (inasmuch as $|\varepsilon_2| \gg |\varepsilon_1|$), Eq. (8) leads to the simple result $T_1 \approx \exp(-L/L_{\text{SPP}})$ in this limit.

To illustrate the developed model, we consider the Ag–air–Ag waveguide with the following set of parameters: $L = 400$ nm, $h = w = 50$ nm, and $d = 300$ nm. We examine the accuracy of the model by calculating the waveguide transmittance with the finite-difference time-domain (FDTD) scheme. In numerical FDTD simulations, we divide the computational domain containing both the MDM-waveguide and the stub into uniform Yee cells with $\Delta x = \Delta y = 2$ nm and surround it by a perfectly absorbing boundary. Figure 4 shows the comparison of our improved analytical model (red curves) with the simulation data (blue curve). For reference, green curves show the transmittance of the waveguide neglecting SPP attenuation due to Ohmic losses (assuming $\text{Im}\,\varepsilon_2 = 0$) and the phase shift due to reflection from the stub end (assuming $Z_L \to \infty$).

#123889 - $15.00 USD Received 5 Feb 2010; revised 23 Feb 2010; accepted 8 Mar 2010; published 11 Mar 2010

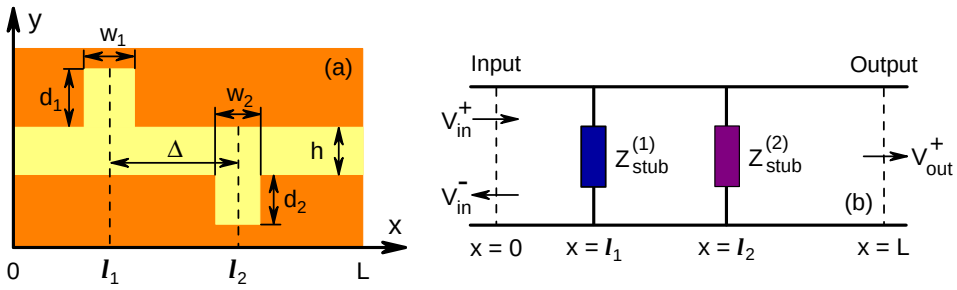

Fig. 5. Schematic of (a) an MDM waveguide coupled to two stubs separated by distance Δ and (b) the corresponding transmission-line model.

In what follows, we use the term "lossless model" to refer to the results obtained under these two assumptions [25, 27]. As is evident from Figure 4, the results of improved model accounting for SPP damping are in good agreement with numerical data. In contrast, the transmission spectrum in the lossless case substantially diverges from the exact one. The disparity between predictions of lossless and improved models becomes worse for longer stubs. This feature is illustrated by the right panel in Fig. 4 for $\lambda = 850$ nm. Notice that, while the transmittance oscillates between 0 and 1 with increasing d in the loss-free case, in the lossy case the amplitude of similar oscillations described by Eq. (8) gradually decays to zero, and the transmittance approaches a constant value of $T_1 = (4/9)\exp(-L/L_{\mathrm{SPP}})$ as $d \to \infty$.

3.2. *Double-stub case*

It is possible to introduce extra degrees of freedom in the design of MDM-waveguide-based optical filters by adding more stubs to the waveguide. The case of two stubs is of particular interest since it admits simple analytical investigation and helps us to better understand the peculiarities of more complex filter geometries. To study the waveguide transmittance in this configuration, we consider the structure shown in Fig. 5(a). For generality of the treatment, we assume that the stubs are different and coupled to the waveguide at points $x = l_1$ and $x = l_2 > l_1$.

Similar to the single-stub case, we replace the MDM waveguide with two stubs by an equivalent transmission line shown in Fig. 5(b). As before, the jth stub in Fig. 5(a) $(j = 1, 2)$ is represented by an effective impedance in the line

$$Z^{(j)}_{\mathrm{stub}} = Z_S(w_j)\,\frac{Z_L(w_j) - iZ_S(w_j)\tan[\beta(w_j)d_j]}{Z_S(w_j) - iZ_L(w_j)\tan[\beta(w_j)d_j]}, \tag{9}$$

where w_j and d_j are the width and length of the jth stub and the functions $Z_S(w_j)$ and $Z_L(w_j)$ are given by Eqs. (3) and (4), respectively. Denoting by $\Delta = l_2 - l_1$ the distance between the stubs, we can write the transfer matrix of the equivalent transmission line as

$$\mathbf{T} = \mathbf{A}(l_1)\mathbf{B}(Z^{(1)}_{\mathrm{stub}})\mathbf{A}(\Delta)\mathbf{B}(Z^{(2)}_{\mathrm{stub}})\mathbf{A}(L - l_2).$$

Using this result in Eq. (6), we find the transmittance of the MDM waveguide coupled to two stubs, $T_2 = |V^+_{\mathrm{out}}/V^+_{\mathrm{in}}|^2$, in the form

$$T_2 = \left|\left(1 + \frac{Z_{\mathrm{MDM}}}{2Z^{(1)}_{\mathrm{stub}}}\right)\left(1 + \frac{Z_{\mathrm{MDM}}}{2Z^{(2)}_{\mathrm{stub}}}\right) - \frac{Z^2_{\mathrm{MDM}}}{4Z^{(1)}_{\mathrm{stub}}Z^{(2)}_{\mathrm{stub}}}\exp(2i\beta\Delta)\right|^{-2}\exp\left(-\frac{L}{L_{\mathrm{SPP}}}\right). \tag{10}$$

This solution shows how the transmittance is affected by the stubs' separation Δ. By comparing T_1 and T_2, we conclude that the first term under the modulus sign in Eq. (10) describes frequency

#123889 - $15.00 USD Received 5 Feb 2010; revised 23 Feb 2010; accepted 8 Mar 2010; published 11 Mar 2010

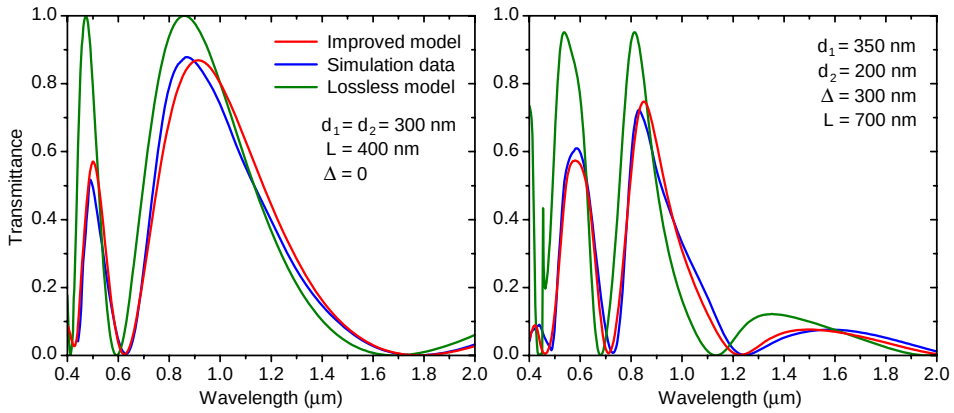

Fig. 6. Comparison between the analytic (red and green curves) and numerically calculated (blue curves) transmission spectra of the Ag–air–Ag-waveguide shown in Fig. 5(a). The left and right panels correspond to identical and different stubs, respectively. In all cases, $w = h = 50$ nm.

response of independent stubs, whereas the second term accounts for multipath interference between waves reflected from the stubs and therefore can be attributed to their "interaction." The interaction strength decays exponentially with Δ making the stubs nearly independent of each other for $\Delta \gg L_{\mathrm{SPP}}$.

If the stubs of equal dimensions ($Z_{\mathrm{stub}}^{(1)} = Z_{\mathrm{stub}}^{(2)} \equiv Z_{\mathrm{stub}}$) are coupled symmetrically at the same location (i.e., $\Delta = 0$), Eq. (10) reduces to

$$T_2 = \left| 1 + \frac{Z_{\mathrm{MDM}}}{Z_{\mathrm{stub}}} \right|^{-2} \exp\left(-\frac{L}{L_{\mathrm{SPP}}} \right). \tag{11}$$

In the PEC approximation, this equation reduces to the well-known result of Ref. [25].

Figure 6 shows numerical examples of the transmission spectra described by Eqs. (10) and (11). The red curves include damping of SPPs through the complex-valued permittivity $\varepsilon_2(\omega)$, the green curves correspond to the lossless model for which $\mathrm{Im}\,\varepsilon_2 = 0$ and $Z_L = \infty$, and the blue curves show T_2 obtained with the FDTD method. As can be seen, the agreement between the results of improved analytical model and FDTD simulations is excellent. Our model not only describes the positions of spectral windows accurately, but it also gives their peak values precisely. In particular, it is capable of accurately reproducing the results of all numerical simulations in Ref. [26]. The lossless model fails to predict true values of the spectral maxima but still allows one to estimate their positions. Notice that, in the asymmetric-stub configuration (right panel), unity transmittance is not always achieved even when the losses are negligible. This simply reflects the fact that transmission through MDM waveguide with stub structure is a coherent process and requires phase matching among the incident and reflected waves to realize a maximum for T_2.

In the absence of losses and the phase shift resulting from SPP reflection, the phase-matching conditions can be readily derived by examining Eq. (10) in the special case $w_1 = w_2 = h$ and using $Z_{\mathrm{MDM}}/Z_{\mathrm{stub}}^{(j)} = -i\tan(\beta d_j)$. If there is only one stub, the transmission T_1 reaches 1, irrespective of the stub length d, at frequencies ω_n satisfying the relation $\beta(\omega_n)d = \pi n$ $(n = 1, 2, 3, \ldots)$. In the presence of two stubs, however, the equality $T_2(\omega_n) = 1$ can be achieved only for a specific relation between d_1, d_2, and Δ. In that instance, the phase-matching conditions are given

#123889 - $15.00 USD Received 5 Feb 2010; revised 23 Feb 2010; accepted 8 Mar 2010; published 11 Mar 2010

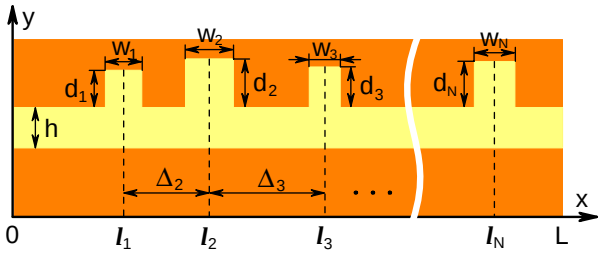

Fig. 7. Schematic of MDM waveguide coupled to N stubs. The position, width, and length of the jth stub are given by l_j, w_j, and d_j, respectively; Δ_j is the distance between $(j-1)$th and jth stubs.

by

$$\beta(\omega_n)(d_1+d_2)=\pi Pn \quad \text{for} \quad \Delta=\frac{p}{q}(d_1+d_2) \quad \text{and}$$
$$\beta(\omega_n)d_1=\pi Qn \quad \text{for} \quad \frac{d_1}{d_2}=\frac{q}{p},$$

where $n=1,2,3,\ldots$ and P and Q are the minimum values of integers $p\neq 0$ and $q\neq 0$ for which the preceding relations among d_1, d_2, and Δ are satisfied. For $\Delta=0$, the first relation formally leads to $q=\infty$ and $P=1$ resulting in $\beta(\omega_n)(d_1+d_2)=\pi n$.

Similar conditions, although not discussed here, may be easily obtained for the loss-free waveguides (with $\mathrm{Im}\,\varepsilon_2=0$) using Eq. (9) of our model. If the metal losses are not negligible, analytic expressions for the phase-matching conditions do not exist. In this instance, analytical conditions for the lossless model together with the dispersion law (1) can be employed to estimate the optimal filter parameters.

4. Transmittance of MDM waveguide with arbitrary stub structure

In this section, we consider how to calculate the transmission spectra in the general case in which an MDM waveguide is coupled to N different stubs at different locations as shown in Fig. 7. As before, the jth stub is characterized by three geometrical parameters l_j, w_j, and d_j. The transfer matrix of the waveguide shown in Fig. 7 can be written in the form

$$\mathbf{T}=\mathbf{A}(l_1)\mathbf{B}(Z^{(1)}_{\mathrm{stub}})\left(\prod_{j=2}^{N}\mathbf{A}(\Delta_j)\mathbf{B}(Z^{(j)}_{\mathrm{stub}})\right)\mathbf{A}(L-l_N), \tag{12}$$

where $Z^{(j)}_{\mathrm{stub}}$ is given in Eq. (9) and $\Delta_j=l_j-l_{j-1}$. Using this result as well as Eqs. (2)–(4), (7), and (9) in Eq. (6), we can find the output voltage, V^+_{out} for given values of input voltage, V^+_{in} and the SPP frequency ω. From the ratio of these voltages, we can obtain the transmittance of an MDM waveguide with arbitrary configuration of N different stubs using $T_N(\omega)=|V^+_{\mathrm{out}}(\omega)/V^+_{\mathrm{in}}|^2$. The values of T_N calculated with this method will be accurate as long as the stubs' separations are much longer than the skin depth of the SPP modes, i.e.,

$$\min_{j\in[2,N]}\Delta_j \gg \frac{2}{|\mathrm{Im}\,k_2|}.$$

In general, Eq. (6) need to be solved numerically. However, if the stubs are arranged periodically, the transmission spectra of the MDM waveguide can be calculated analytically. As an

#123889 - $15.00 USD Received 5 Feb 2010; revised 23 Feb 2010; accepted 8 Mar 2010; published 11 Mar 2010

example, we consider the simplest case of N identical stubs spaced apart by a distance Δ. After some tedious but straightforward algebra, we arrive at the following expression:

$$T_N = \left|\Phi_+^{N-1} G_+ - \Phi_-^{N-1} G_-\right|^{-2} \exp\left(-\frac{L}{L_{\mathrm{SPP}}}\right), \tag{13}$$

where

$$\Phi_\pm = \frac{1}{2}\left[1 + \frac{Z_{\mathrm{MDM}}}{2Z_{\mathrm{stub}}} + \left(1 - \frac{Z_{\mathrm{MDM}}}{2Z_{\mathrm{stub}}}\right)\exp(2i\beta\Delta) \pm Q\right],$$
$$G_\pm = \frac{1}{2Q}\left\{\left(1 + \frac{Z_{\mathrm{MDM}}}{2Z_{\mathrm{stub}}}\right)^2 - \left[1 + \left(\frac{Z_{\mathrm{MDM}}}{2Z_{\mathrm{stub}}}\right)^2\right]\exp(2i\beta\Delta)\right\} \pm \frac{1}{2}\left(1 + \frac{Z_{\mathrm{MDM}}}{2Z_{\mathrm{stub}}}\right),$$
$$Q = \left\{\left[1 + \frac{Z_{\mathrm{MDM}}}{2Z_{\mathrm{stub}}} + \left(1 - \frac{Z_{\mathrm{MDM}}}{2Z_{\mathrm{stub}}}\right)\exp(2i\beta\Delta)\right]^2 - 4\exp(2i\beta\Delta)\right\}^{1/2}.$$

It is easy to verify by direct evaluation of Eq. (13) that, for $N = 1$ and $N = 2$, it reduces, respectively, to Eq. (8) and Eq. (10) with $Z_{\mathrm{stub}}^{(1)} = Z_{\mathrm{stub}}^{(2)}$. In the case of widely separated stubs ($\Delta \gg L_{\mathrm{SPP}}$), the terms containing exponents in the functions $\Phi_\pm$, $G_\pm$, and Q vanish, and transmittance takes the simple form

$$T_N = \left|1 + \frac{Z_{\mathrm{MDM}}}{2Z_{\mathrm{stub}}}\right|^{-2N} \exp\left(-\frac{L}{L_{\mathrm{SPP}}}\right).$$

This result can be interpreted as the transmittance of N successive noninteracting waveguides each of which is coupled to one stub. As before, the term "noninteracting" implies that the interference between the waves reflected from different stubs can be neglected.

Another situation that is interesting to analyze using Eq. (13) arises when the stubs form a Bragg grating with a specific period $\Delta = \lambda/(2\mathrm{Re}\, n_{\mathrm{eff}}) = \lambda_{\mathrm{MDM}}/2$. In the absence of losses, this situation is characterized by the condition $\beta\Delta = \pi$, whose use reduces Eq. (13) to

$$T_N = \left|1 + N\frac{Z_{\mathrm{MDM}}}{2Z_{\mathrm{stub}}}\right|^{-2} = \left\{1 + \frac{N^2}{4}\left[\frac{\sqrt{\varepsilon_1} + \sqrt{|\varepsilon_2|}\tan(\pi d/\Delta)}{\sqrt{|\varepsilon_2|} + \sqrt{\varepsilon_1}\tan(\pi d/\Delta)}\right]^2\right\}^{-1}. \tag{14}$$

In deriving this equation, we assumed $w = h$ and employed Eq. (9). It is easy to see that the transmissivity becomes 100% ($T_N = 1$) for

$$\frac{d}{\Delta} = n - \frac{1}{\pi}\tan^{-1}\sqrt{\frac{\varepsilon_1}{|\varepsilon_2|}},$$

where $n = q, q+1, q+2, \ldots$, $q = \lceil (1/\pi)\tan^{-1}(\varepsilon_1/|\varepsilon_2|)^{1/2}\rceil$, and the sign "$\lceil\ldots\rceil$" stands for the ceiling function. For a large number of stubs, the transmission peaks with full-width at half-maximum (FWHM) $\delta \approx 4(\pi N)^{-1}(|\varepsilon_2| - \varepsilon_1)/(|\varepsilon_2| + \varepsilon_1)$ are separated by broad stop bands with $T_N \approx 0$ in which the MDM waveguides acts as a reflector. If the losses are not negligible but $\Delta \ll L_{\mathrm{SPP}}$, the first part of Eq. (14) can still be used to calculate the transmittance when $\mathrm{Re}\beta\Delta = \pi$, provided that the factor $\exp(-L/L_{\mathrm{SPP}})$ is introduced. Qualitatively speaking, the presence of losses shifts the position of the stop bands and reduces the peak values of T_N.

To illustrate the accuracy of our model, we consider two numerical examples in Fig. 8 with the parameter values given there. More specifically, this figure shows the transmittance of MDM waveguides coupled to 3 and 4 stubs. The stubs are assumed to be identical and have the same width as the waveguide, which is often the case in practice. The analytical results obtained from

#123889 - $15.00 USD Received 5 Feb 2010; revised 23 Feb 2010; accepted 8 Mar 2010; published 11 Mar 2010

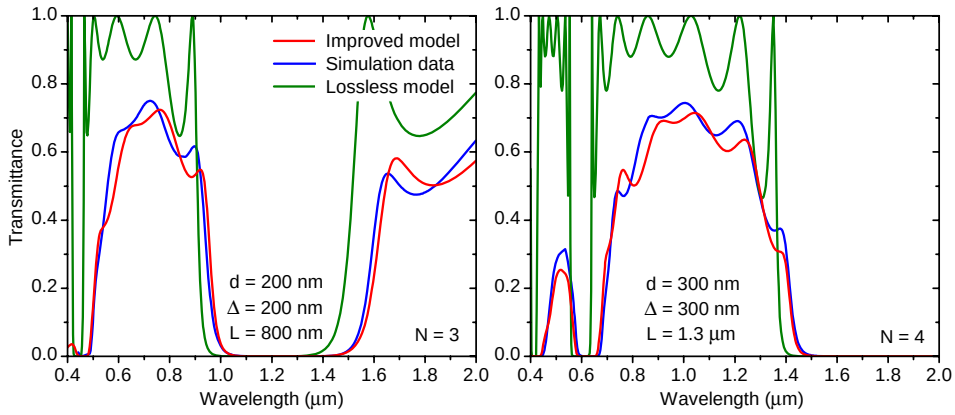

Fig. 8. Transmittance of Ag–air–Ag-waveguide as a function of frequency for three (left panel) and four (right panel) equal stubs coupled perpendicular to the waveguide axis. In both panels, $h = w = 50$ nm.

Eq. (13) (red curves) agree well with the numerical FDTD data (blue curves); spectra for the lossless model (green curves) are also shown for comparison. Specifically, both the positions of the spectra pass-bands and the transmittances within them are reproduced fairly well by our improved analytical model. In contrast, the transmission spectra of lossless model deviate significantly from the real ones. As the waveguide length and/or the number of stubs increase, the predictions of the lossless model that neglects SPP damping and the reflection-induced phase shift become worse.

It should be emphasized that our analytical model produces acceptable results much faster compared with full-scale FDTD simulations. For example, the times required to obtain blue and red spectra in Fig. 8 approximately differ by a factor of 10^5. Such a considerable reduction in computational time and the accuracy attainable with our analytical scheme suggest that our model can be used as a powerful tool for designing and optimizing MDM-waveguide-based photonic devices.

5. Summary

In this work, we developed an improved theoretical model which describes transmission through metal-dielectric-metal (MDM) waveguides with an arbitrary stub structure and includes losses incurred during propagation of SPPs along the two metal-dielectric interfaces. We have shown that our model admits analytical solutions for a number of practically-important stub geometries. The model employs the physical similarity of MDM waveguides coupled to multiple stubs and standard transmission lines with lumped impedances. To take advantage of this similarity, we established a mapping between the optical parameters of MDM waveguides and the impedances representing stubs. It is essential that, in doing so, we take proper account of dissipative losses described by the complex-valued dielectric permittivities of the waveguide constituents. Our model accounts not only for ohmic losses of metals but also for the phase shift resulting from SPP reflections from the stubs' ends. Using the proposed model, we derived explicit expressions for the transmission spectra of MDM waveguides coupled to one stub, two unequal stubs, and arbitrary number of equal stubs arranged periodically.

We validated our analytical model by comparing its predictions with numerical FDTD simulations for several MDM waveguides with different stub configurations. We showed that our model is capable of predicting precise transmission spectra that can be calculated much faster

#123889 - $15.00 USD Received 5 Feb 2010; revised 23 Feb 2010; accepted 8 Mar 2010; published 11 Mar 2010

($>$ 10 000 times) compared with the FDTD method. Our model and analytical results should prove useful in designing and optimizing MDM-waveguide-based optical components. In particular, the analysis of the derived formulae reveals the ways to engineer the transmission spectra of MDM-waveguide-based optical filters.

Acknowledgment

This work was partially funded by the Australian Research Council through its Discovery Grant scheme under grant DP0877232. The work of G. P. Agrawal is also supported by the U.S. National Science Foundation award ECCS-0801772.

#123889 - $15.00 USD Received 5 Feb 2010; revised 23 Feb 2010; accepted 8 Mar 2010; published 11 Mar 2010